J|A|C|S
ARTICLES
Published on Web 06/14/2006

Unveiling the "Booster Effect" of Fluorinated Alcohol Solvents: Aggregation-Induced Conformational Changes and Cooperatively Enhanced H-Bonding

Albrecht Berkessel,* Jens A. Adrio, Daniel Hüttenhain, and Jörg M. Neudörfl

Contribution from the Institut für Organische Chemie, Universität zu Köln, Greinstrasse 4, D-50939 Köln, Germany

Received July 8, 2005; Revised Manuscript Received May 1, 2006; E-mail: berkessel@uni-koeln.de

Abstract: The influence of conformation and aggregation on the hydrogen bond donor ability of fluorinated alcohol solvents [1,1,1,3,3,3-hexafluoro-2-propanol (HFIP) and 1-phenyl-2,2,2-trifluoroethanol (PhTFE)] was explored theoretically (DFT) and experimentally (NMR, kinetics, crystal structure analyses). The detailed DFT analysis revealed a pronounced dependence of the H-bond donor ability on the conformation along the CO-bond of the monomeric alcohols. The donor orbital energy (σ^*_{OH}) decreases and the molecular dipole moment (μ) increases drastically from the antiperiplanar (ap) to the synperiplanar (sp) H_CCOH conformation. The kinetics of olefin epoxidation with H_2O_2 in HFIP indicate higher order solvent aggregates (2−3 monomers) to be responsible for the activation of the oxidant. Single-crystal X-ray analyses of HFIP and PhTFE confirmed the existence of H-bonded aggregates (infinite helices, ribbons, and cyclic oligomers) and the predominance of sc to sp conformations of the fluoroalcohol monomers. These aggregate structures served as the basis for a DFT analysis of the H-bond donor ability at the terminal hydroxyl group of HFIP mono- to pentamers. Both the LUMO energy and the natural charge of the terminal hydroxyl proton indicated a substantial cooperative influence of dimerization and trimerization on the H-bond donor ability. We therefore conclude that dimers and trimers, with the individual monomers in their sc to sp conformation, play a crucial role for the solvolytic and catalytic effects exerted by HFIP, rather than monomers.

I. Introduction

Fluorinated alcohols such as 2,2,2-trifluoroethanol (TFE), 1,1,1,3,3,3-hexafluoro-2-propanol (HFIP), or 1-phenyl-2,2,2-trifluoroethanol (PhTFE) have remarkable solvent properties which clearly distinguish them from their nonfluorinated analogues.

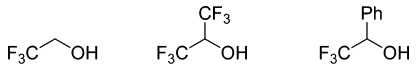

TFE **HFIP** **PhTFE**

For example, they denature the native structure of proteins and induce helicity in peptides.[1,2] Our interest in fluorinated alcohols was triggered by the fact that they are exceptional solvents for a variety of reactions,[3] especially oxidations.[4] In HFIP, the rate of epoxidation of olefins by hydrogen peroxide is raised by as much as 5 orders of magnitude, compared to conventional solvents.[5] Their strong H-bond donor ability was discussed as one major cause for the dramatically enhanced reactivity.[6,7] On the other hand, based on kinetic,[5] spectroscopic,[2] and molecular dynamics studies,[8] it has been argued that the observed effects are not brought about by the fluorinated alcohol in its monomeric form but rather by higher order aggregates. To shed light on the intriguing "HFIP phenomena", we initiated a combined computational and experimental analysis aiming at a better understanding of (i) the conformation−activity relation of monomeric fluoroalcohols, especially their H-bond donor ability, (ii) the alteration of these properties upon aggregation, and (iii) the difference to nonfluorinated analogues.

II. Results

II.a. HFIP as an H-Bond Donor to Ethers. To investigate the exceptional hydrogen-bond donor ability of fluorinated alcohols, we examined, by NMR titration, the formation of complexes of HFIP with several ethers. The titration was accomplished by successively adding the hydrogen bond ac-

(1) Andersen, N. H.; Dyer, R. B.; Fesinmeyer, R. M.; Gai, F.; Liu, Z. H.; Neidigh, J. W.; Tong, H. *J. Am. Chem. Soc.* **1999**, *121*, 9879−9880. Mulla, H. R.; Cammers-Goodwin, A. *J. Am. Chem. Soc.* **2000**, *122*, 738−739. Cammers-Goodwin, A.; Allen, T. J.; Oslick, S. L.; McClure, K. F.; Lee, J. H.; Kemp, D. S. *J. Am. Chem. Soc.* **1996**, *118*, 3082−3090.
(2) Hong, D.-P.; Hoshino, M.; Kuboi, R.; Goto, Y. *J. Am. Chem. Soc.* **1999**, *121*, 8427−8433.
(3) Bégué, J. P.; Bonnet-Delpon, D.; Crousse, B. *Synlett* **2004**, 18−29.
(4) Ravikumar, K. S.; Zhang, Y. M.; Bégué, J.-P.; Bonnet-Delpon, D. *Eur. J. Org. Chem.* **1998**, *1998*, 2937−2940. Ravikumar, K. S.; Bégué, J.-P.; Bonnet-Delpon, D. *Tetrahedron Lett.* **1998**, *39*, 3141−3144. Neimann, K.; Neumann, R. *Org. Lett.* **2000**, *2*, 2861−2863. van Vliet, M. C. A.; Arends, I. W. C. E.; Sheldon, R. A. *Synlett* **2001**, 248−250. Berkessel, A.; Andreae, M. R. M. *Tetrahedron Lett.* **2001**, *42*, 2293−2295. Berkessel, A.; Andreae, M. R. M.; Schmickler, H.; Lex, J. *Angew. Chem., Int. Ed.* **2002**, *41*, 4481−4484.
(5) Berkessel, A.; Adrio, J. A. *Adv. Synth. Catal.* **2004**, *346*, 275−280.
(6) de Visser, S. P.; Kaneti, J.; Neumann, R.; Shaik, S. *J. Org. Chem.* **2003**, *68*, 2903−2912.
(7) Ben-Daniel, R.; de Visser, S. P.; Shaik, S.; Neumann, R. *J. Am. Chem. Soc.* **2003**, *125*, 12116−12117.
(8) Fioroni, M.; Burger, K.; Mark, A. E.; Roccatano, D. *J. Phys. Chem. B* **2001**, *105*, 10967−10975.

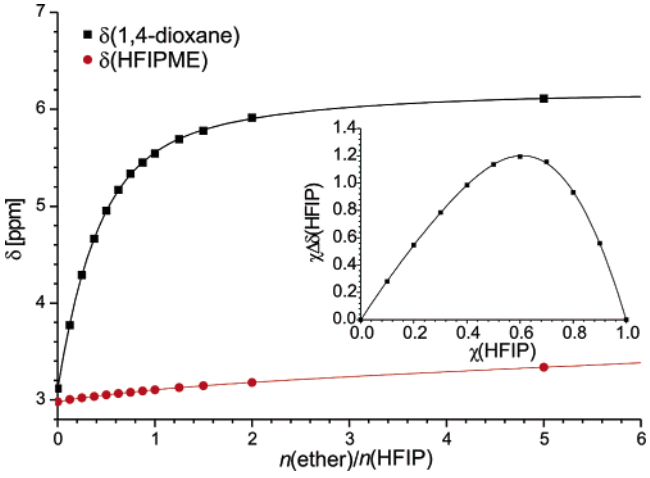

Figure 1. NMR titration curves of HFIP with 1,4-dioxane and HFIPME. Inset: Job plot of the complex formation of HFIP and 1,4-dioxane in $CDCl_3$ at 25 °C.

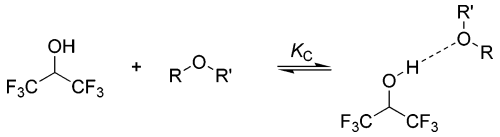

Figure 2. General complexation equilibrium of HFIP with ethers.

ceptor compound to an NMR sample of HFIP and determining the change in the chemical shift δ of the hydroxyl proton. A significant downfield shift of the alcoholic proton was observed in the ^{1}H NMR with increasing concentration of 1,4-dioxane (Figure 1). This fact clearly indicates the formation of a hydrogen bonded complex with an association constant K_C (Figure 2). Only one hydroxyl proton signal was observed, indicative of a fast equilibrium on the NMR time scale.

$$K_C = [\text{complex}]/[\text{HFIP}]\cdot[\text{ether}]$$

The complexation constants K_C were determined from the NMR titrations to be 33 L mol^{-1} for 1,4-dioxane and 0.76 L mol^{-1} for 1,1,1,3,3,3-hexafluoro-2-propyl-methyl ether (HFIPME), based on the Rose−Drago method.[9] This proves the strong complexation of HFIP with cyclic ethers such as 1,4-dioxane in contrast to the very weak interaction with HFIPME.[10]

Further evidence for the complexation of HFIP by 1,4-dioxane was obtained by NOESY experiments at a 1:1 ratio of HFIP and the particular acceptor. A strong intermolecular NOE was observed between the methylene protons of 1,4-dioxane and the two HFIP protons. In contrast, no NOE was observed between the C−H proton of HFIP and any proton of HFIPME. To determine the stoichiometry of the HFIP/1,4-dioxane complex, another set of ^{1}H NMR spectra with a constant total concentration of H-bond donor and acceptor was recorded. The resulting Job plot (Figure 1, inset) shows a maximum at an HFIP molar fraction of 0.61, suggesting a complexation ratio HFIP/1,4-dioxane of 1.6:1.[11] This result indicates a strong first complexation and a weaker second one.

II.b. Kinetics of Olefin Epoxidation with Hydrogen Peroxide in HFIP. As a second experimental probe, we analyzed the kinetics of the epoxidation of *Z*-cyclooctene by hydrogen peroxide in HFIP as the solvent. As reported earlier, the reaction kinetics clearly show a first-order dependence on substrate and oxidant, suggesting a monomolecular participation of these components in the rate determining step.[5] With respect to the fluorinated alcohol, we initiated four sets of experiments. In each set of experiments (i−iv), a series of epoxidation reactions was run in mixtures of HFIP with a cosolvent inert to the oxidative reaction conditions. Keeping the total reaction volume constant, the HFIP concentration was attenuated by the addition of chloroform (i), 1,2-dichloroethane (ii), HFIPME (iii), and 1,4-dioxane (iv).[5] Whereas 1,4-dioxane is miscible with all reaction components over the entire concentration range, from 1,4-dioxane to pure HFIP, the other cosolvents could only be used in mixtures with more than ca. 40% (v/v) HFIP to avoid phase separation. The relative reaction rates[12] k_{rel} were monitored as a function of the HFIP concentration. In all cases, a substantial decrease in epoxidation rate was detected with decreasing concentrations of HFIP, most severely with 1,4-dioxane as cosolvent. This is in line with the assumption that the hydrogen bond donor ability of HFIP is vital for the catalytic activity. A strong hydrogen bond acceptor such as 1,4-dioxane competes with the "active epoxidation pathway" for the fluoroalcohol (Figure 3).

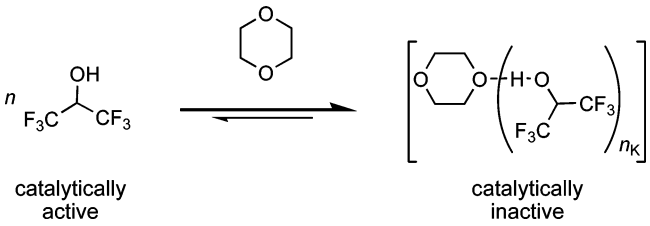

Figure 3. Deactivation of HFIP by H-bonding with 1,4-dioxane.

The kinetic rate order in HFIP can be extracted from the slope of a doubly logarithmic plot of the reaction rate as a function of the HFIP concentration (Figure 4). For the chloroalkane cosolvents, we found a kinetic rate order of 2 to 3. This kinetic order suggests a more complex participation of HFIP in the rate determining step than previously assumed by Shaik et al.[6]

The most suitable cosolvent for the evaluation of the kinetic rate order in HFIP is the methyl ether derivative of HFIP: (i) HFIPME is similar to HFIP with respect to the polarity ($\epsilon_{HFIP} = 17.8$,[8] $\epsilon_{HFIPME} = 15.4$[13]), and (ii) HFIPME is the most appropriate analogue of HFIP with respect to its H-bond *acceptor* capacity. The only property this cosolvent misses is exactly the one decisive for catalytic activity: the hydrogen bond *donor* ability. Employing HFIPME as cosolvent, we determined a kinetic rate order in HFIP for the epoxidation of *Z*-cyclooctene of almost 3 ($m = 2.72 \pm 0.15$; Figure 4b).

In the case of 1,4-dioxane as cosolvent, we earlier reported a rate law exponent of $m = 12 \pm 1$.[5] However, since the reaction is catalyzed only by non-ether bound HFIP (Figure 3), we accounted for this by the complexation equilibrium between HFIP and 1,4-dioxane (section II.a). Plotting the epoxidation

(9) Rose, N. J.; Drago, R. S. *J. Am. Chem. Soc.* **1959**, *81*, 6138−6141. Hirose, K. *J. Inclusion Phenom. Macrocyclic Chem.* **2001**, *39*, 193−209.
(10) See the Supporting Information for a more detailed compilation of experimentally determined complexation constants and correlation with available literature data.
(11) Job, P. *Ann. Chim.* **1928**, *113*, 113−116. Huang, C. Y. *Methods Enzymol.* **1982**, *87*, 509−525.
(12) Reaction rates k_{rel} correspond to the rate constants k_i at a given HFIP concentration relative to the rate constant of the reaction in pure HFIP.
(13) Nakazawa, N.; Kawamura, M.; Sekiya, A.; Ootake, K.; Tamai, R.; Kurokawa, Y.; Murata, J. *Trans. of the JSRAE* **2001**, *18*, 263−271.

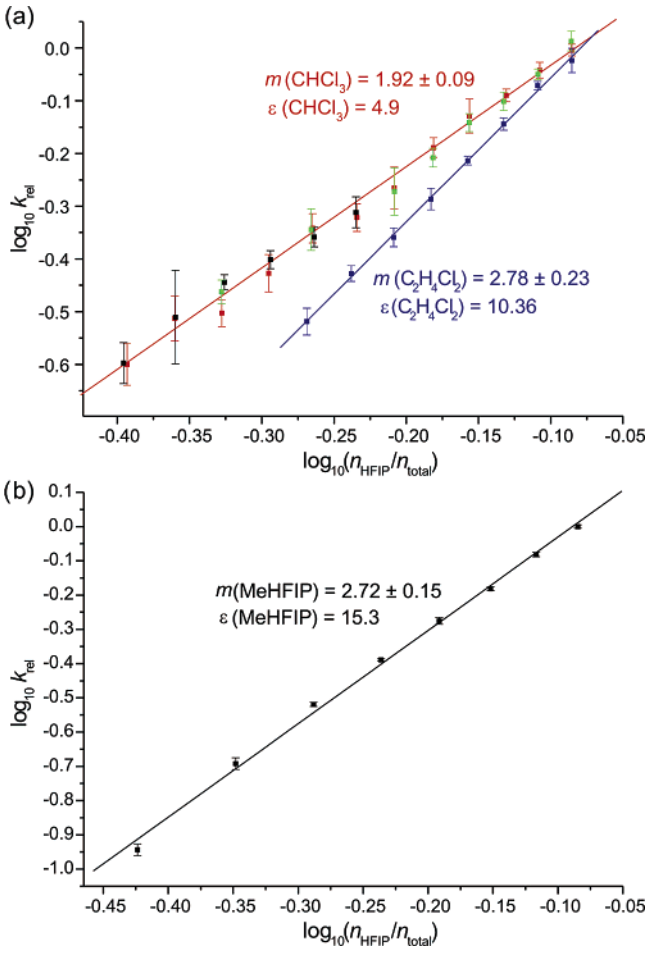

Figure 4. Correlation between the epoxidation rate of *Z*-cyclooctene (**1**) and the molar fraction of HFIP with chloroform and 1,2-dichloroethane (a) as well as HFIPME (b) as cosolvents.

rate constant as a function of the "free" HFIP concentration (n^{f}_{HFIP}/n_{total}), we again found a third order dependence ($m = 3.0 \pm 0.7$). In summary, we found the kinetic rate order in HFIP to be 2 to 3 for all cosolvents tested. We therefore suggest 2 to 3 molecules of HFIP to be involved in the rate limiting step of the kinetically dominant reaction path for oxygen transfer from H_2O_2 to the olefin.

II.c. Conformational Analysis of Monomeric Fluorinated Alcohols. Of all conformational parameters in HFIP, the preferred dihedral angle along the CO-bond, i.e., the H_CCOH torsion angle, has been of prime interest.[14,15] Based on jet expansion FT-IR spectroscopy and ab initio calculations, Suhm et al.[15] concluded that the most populated conformer of the HFIP monomer carries the OH group antiperiplanar (ap) to the adjacent CH. This conformer is approximately 1 kcal/mol more stable than the synclinal (sc) one. The question results whether it is HFIP in this very conformation that is responsible for the unique behavior, e.g., as a H-bond donor in the liquid phase. The attractive interaction of hydrogen bonding is effected mainly by electrostatic and donor-acceptor/charge-transfer ($n_{Acc} \rightarrow \sigma^*_D$) contributions.[16−20] There is strong evidence that the covalent character of H-bonding becomes increasingly important the stronger and the shorter the interaction is.[18,19] This should be of particular importance for the catalysis of reactions where HFIP stabilizes highly polar transition states via hydrogen bond donation. Shaik et al.[6] have demonstrated for epoxidation reactions that the H-bond from HFIP to H_2O_2 is shortened by an additional 0.24 Å in the course of the oxygen transfer, compared to the equilibrium distance $r_{OH-O} = 1.87$ Å in the preceding H_2O_2−HFIP complex. Also the cooperativity of H-bonding is most easily understood in terms of a covalent charge-transfer interaction.[17]

As a measure for the H-bond donor ability, we analyzed the frontier acceptor orbital energy, that is the lowest unoccupied MO with a substantial antibonding character of the hydroxyl (denoted σ^*_{OH}). The charge-transfer stabilization, on interaction with an arbitrary acceptor, is expected to become stronger the closer the potential donor and acceptor orbitals are in energy.[20] Additionally, the dipole moment and the partial atomic charges at the hydroxyl proton were determined as the decisive factors for the electrostatic H-bonding contributions. In the case of the alcohol monomer, we were particularly interested in the dependence of these parameters on the conformation.

II.c.1. Computational Details for the Conformational Analysis of Fluorinated Alcohols: Single parameter constrained or full geometry optimizations as well as vibrational analyses were performed with the hybrid B3LYP functional as implemented in the Gaussian03 suite of programs[21] in combination with the 6-31+G(d,p) split valence basis set. In the case of HFIP, additional unconstrained geometry optimizations in the gas phase and within a PCM (see below) were run with the more flexible cc-pVTZ basis. For subsequent energetic and orbital evaluations of the B3LYP/6-31+G(d,p) structures, refined single-point computations with the more extensive 6-311++G(d,p) basis set were conducted. Partial atomic charges are based on an NBO analysis.[18] The dipole moment of HFIP was further evaluated, utilizing the POL basis set specifically designed by Sadlej[22] for the calculation of field response properties. Since the aim of this work was to elucidate the structure/activity relation of fluorinated alcohols in the liquid phase, we were interested to include the effects of the nonspecific solvation on the monomer properties. Therefore, the gas phase structures of HFIP optimized at B3LYP/6-31+G(d,p) were embedded in a polarized continuum using the integral equation formalism (IEFPCM).[21,23] We chose acetone as a model solvent for HFIP, as it has a dielectric constant most similar to that of HFIP within the set of implemented solvents ($\epsilon_r = 20.7$ for acetone; $\epsilon_r = 17.8$ for HFIP[8]).

II.c.2. Results of the Conformational Analysis of the Alcohol Monomers: In agreement with Suhm et al.,[15] we identified HFIP in the two sc conformations to be ca.

(14) Truax, D. R.; Wieser, H.; Lewis, P. N.; Roche, R. S. *J. Am. Chem. Soc.* **1974**, *96*, 2327−2338.
(15) (a) Schaal, H.; Häber, T.; Suhm, M. A. *J. Phys. Chem. A* **2000**, *104*, 265−274. (b) Maiti, N. C.; Carey, P. R.; Anderson, V. E. *J. Phys. Chem. A* **2003**, *107*, 9910−9917.
(16) Morokuma, K. *Acc. Chem. Res.* **1977**, *10*, 294−300. Singh, U. C.; Kollman, P. A. *J. Chem. Phys.* **1984**, *80*, 353−355. Dannenberg, J. J.; Haskamp, L.; Masunov, A. *J. Phys. Chem. A* **1999**, *103*, 7083−7086.
(17) King, B. F.; Weinhold, F. *J. Chem. Phys.* **1995**, *103*, 333−347.
(18) Reed, A. E.; Curtiss, L. A.; Weinhold, F. *Chem. Rev.* **1988**, *88*, 899−926.
(19) Steiner, T. *Angew. Chem., Int. Ed.* **2002**, *41*, 48−76.
(20) Guerra, C. F.; Bickelhaupt, F. M. *J. Chem. Phys.* **2003**, *119*, 4262−4273.
(21) Frisch, M. J. et al. *Gaussian 03*, revision C.02; Gaussian, Inc.: Wallingford, CT, 2004. See Supporting Information for full author list.
(22) Sadlej, A. J. *Collect. Czech. Chem. Commun.* **1988**, *53*, 1995−2016.
(23) Cances, E.; Mennucci, B.; Tomasi, J. *J. Chem. Phys.* **1997**, *107*, 3032−3041. Cossi, M.; Barone, V.; Mennucci, B.; Tomasi, J. *Chem. Phys. Lett.* **1998**, *286*, 253−260. Mennucci, B.; Tomasi, J. *J. Chem. Phys.* **1997**, *106*, 5151−5158.

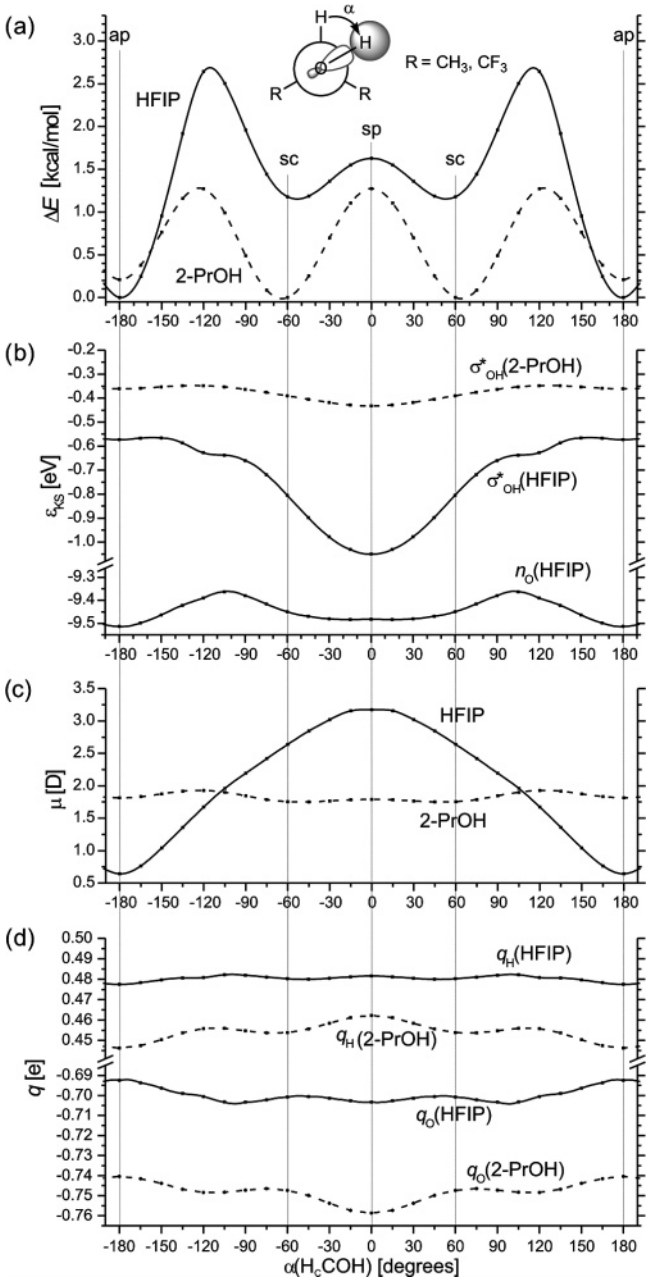

Figure 5. Conformational analysis of HFIP and 2-PrOH in the gas phase: potential energy (a), frontier orbital energies (b), dipole moment (c), and hydroxyl partial charges from an NBO-analysis (d) vs the H_CCOH dihedral angle (B3LYP/6-311++G(d,p)//B3LYP/6-31+G(d,p)).

1 kcal/mol higher in energy (gas phase) than in the ap form (Figure 5a). Interestingly, the σ^*_{OH}-orbital energy in HFIP reacts very sensitively to rotation around the CO-bond, in contrast to the nonfluorinated analogue 2-propanol (Figure 5b). Whereas the σ^*_{OH}-orbital energy difference of the two alcohols is rather small (0.21 eV) in the ap conformation, the energy gap increases dramatically toward the sc (0.46 eV) and even more so the sp conformation (0.62 eV). In contrast, the highest orbital of HFIP with an oxygen lone-pair character (denoted n_O) is not significantly affected. The dipole moment of HFIP also shows a pronounced dependence on the H_CCOH dihedral angle as it increases steadily and drastically from 0.64 D in the ap conformation to 2.74 D in the sc and 3.17 D in the sp form (Figure 5c). However, the electrostatic contribution at short distances is effected mainly by the opposite local atomic

Table 1. Selected H-bond Parameters of Crystal Structures Involving HFIP as H-Bond Donors

ref	d (O_{HFIP}–X_{Acc}) [Å]	α (H_CCOH) [deg]	α (H_CCOX_{Acc})[a] [deg]	
26	2.662	12.5	6.8	(9.9)
27	2.637			(9.6)
	2.797			(45.7)
28	2.632		3.9	(1.5)
29	2.722	0.7	1.0	(0.9)

[a] Values in parentheses correspond to the dihedrals derived under the assumption that H_C is positioned on the bisector of the two $C_{CF3}C_HO$ planes.

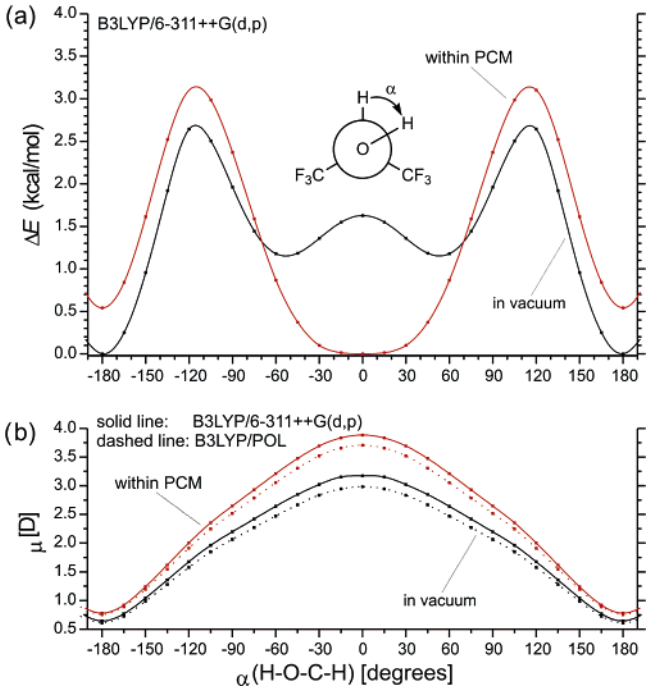

Figure 6. Potential energy (a) and dipole moment (b) of HFIP vs H_CCOH dihedral angle in a vacuum and within a PCM.

charges[20] of the hydroxyl proton q_H and the acceptor heteroatom q_X. Thus, we do not expect electrostatics to be of major importance, as q_H changes by less than 1% (Figure 5d).

From the above we conclude that HFIP mainly exerts its considerable H-bond donor character in an sc or even sp conformation. In fact, this trend is reflected by all crystal structures involving HFIP as a H-bond donor (Table 1).[24] In all cases, the H_CCOH dihedral angle is between 0° and 46°, mostly not exceeding 10°, the region of lowest σ^*_{OH}-orbital energy and highest dipole moment. The same holds for the mechanistic analysis by Shaik,[6] who found a dihedral of 20.6° in the TS of HFIP-assisted epoxidation with H_2O_2. Very similar results were obtained for PhTFE. X-ray crystal structures containing PhTFE as an H-bond donor reveal a distortion of the fluoroalcohols from their monomeric gas phase conformation. The H_CCOH dihedral angles adopted in the crystal structures are characterized by a higher dipole moment and a lower σ^*_{OH}-orbital energy.[25]

Interestingly, the conformational equilibrium is reversed when HFIP is embedded in a polar medium (Figure 6a). Stabilizing the higher dipole moment of the sc or sp conformer, this polar environment significantly alters the potential energy of HFIP,

(24) Allen, F. H. *Acta Crystallogr.* **2002**, *B58*, 380−388.
(25) See Supporting Information for details on the conformational analysis of PhTFE (computations and in X-ray crystal structures).

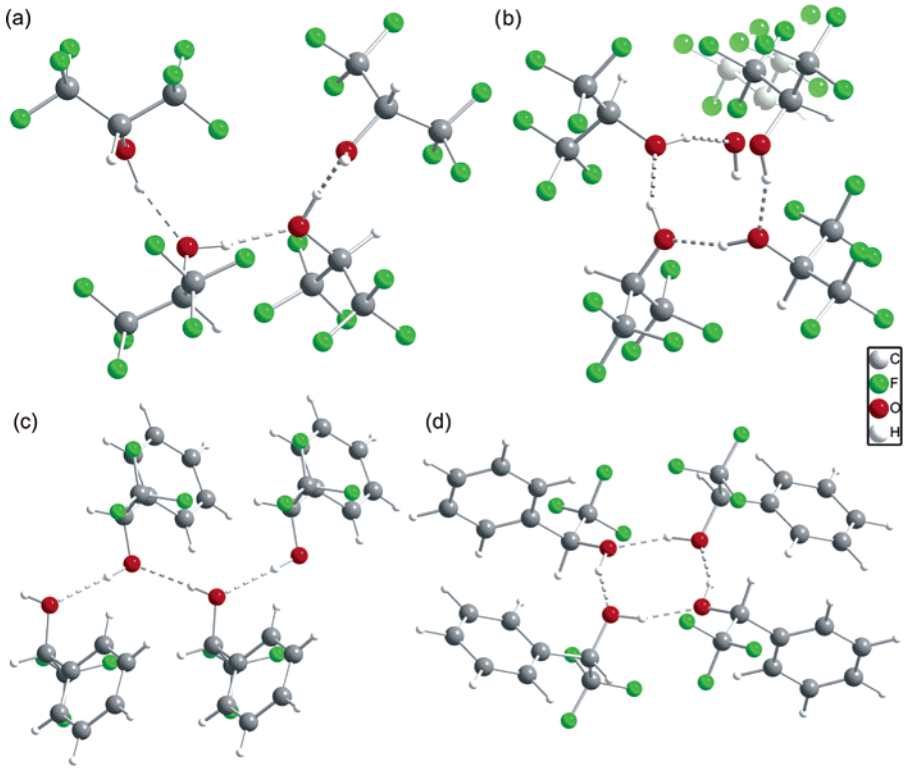

Figure 7. Single-crystal X-ray structures of HFIP ((a) view perpendicular to the helix axis; (b) view along the helix axis), enantiomerically pure PhTFE (c), and racemic PhTFE (d).

Table 2. Conformational, Energetic, and Electronic Properties of the Fully Optimized HFIP Conformers in a Vacuum and within a PCM

	gas phase ($\epsilon_r \equiv 1$)			PCM ($\epsilon_r = 20.7$)		
B3LYP/cc-pVTZ	ap	sc	n_{ap}/n_{sc}	ap	sc	n_{ap}/n_{sc}
α_{HCOH} [deg]	180	56		180	22	
ΔE_{zpve} [kcal/mol]	0	1.07		0.56	0	
ΔG [kcal/mol]	0	1.12	87:13	0.75	0	22:78
μ [D]	0.58	2.46		0.78	3.64	

giving rise to a shallow absolute minimum around synperiplanarity (absolute and relative minimum structure data of HFIP conformers optimized at B3LYP/cc-pVTZ in a vacuum and in a PCM are summarized in Table 2).

II.d. Aggregation of Fluorinated Alcohols: Crystal Structures. We attempted the crystallization of HFIP, as well as enantiopure and racemic PhTFE. In all three cases, we were able to obtain, for the first time, single-crystal X-ray structures (Figure 7). Whereas HFIP and *R*-PhTFE crystallized in infinite helices and zigzag chains, respectively, racemic PhTFE forms cyclic (2*R*+2*S*)-tetramers.

The above X-ray analyses unambiguously established the sc conformation along the CO-bond for both fluorinated alcohols. Thus, from gas phase over liquid phase (as represented by HFIP in the PCM) to the solid state, the conformational equilibrium of HFIP had indeed completely *reversed* from an ap to an sc preference. Upon aggregation, the dihedral is reduced toward the sp conformation for both fluorinated alcohols, with an average H_CCOH torsional angle of 31° for HFIP and −21° for *R*-PhTFE.[30] This is consistent with the above conformational analysis of monomeric HFIP exerting its highest H-bond donor capacity in this form (see Figure 5). The same holds for PhTFE.[25]

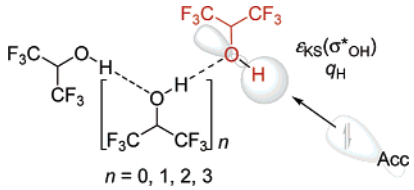

Figure 8. Aggregation-induced H-bonding enhancement of HFIP.

II.e. Aggregation of Fluorinated Alcohols: Computational Analysis. Assuming that solid-state aggregation patterns resemble those in the liquid phase,[31] we investigated the effect of aggregation on the H-bond donor capacity of HFIP. In chains of H-bonded molecules comprising one to five HFIP monomers, we analyzed the H-bond donor ability of the free hydroxyl at the chain end (Figure 8). As the measure for the H-bond donor strength, we again determined the corresponding σ^*_{OH}-orbital energy and the partial charge of the hydroxyl proton.[21]

Computational Details for the Analysis of Alcohol Aggregates: For both alcohols, HFIP and 2-PrOH, the HFIP-helix from the X-ray analysis served as the structural basis of the orbital and NBO evaluation.

HFIP: Helix fragments comprising up to 5 alcohol monomers were subjected to (i) unconstrained geometry optimizations, and

(26) Maekawa, Y.; Kato, S.; Hasegawa, M. *J. Am. Chem. Soc.* **1991**, *113*, 3867−3872.
(27) Ishida, Y.; Aida, T. *J. Am. Chem. Soc.* **2002**, *124*, 14017−14019.
(28) Osakada, K.; Kim, Y. J.; Tanaka, M.; Ishiguro, S.; Yamamoto, A. *Inorg. Chem.* **1991**, *30*, 197−200.
(29) Gonsior, M.; Krossing, I.; Mitzel, N. *Z. Anorg. Allg. Chem.* **2002**, *628*, 1821−1830.
(30) The negative H_CCOH dihedral angle in PhTFE was defined herein as the rotation of the hydroxyl proton towards the CF_3 group.
(31) Ludwig, R. *Angew. Chem., Int. Ed.* **2001**, *40*, 1808−1827.

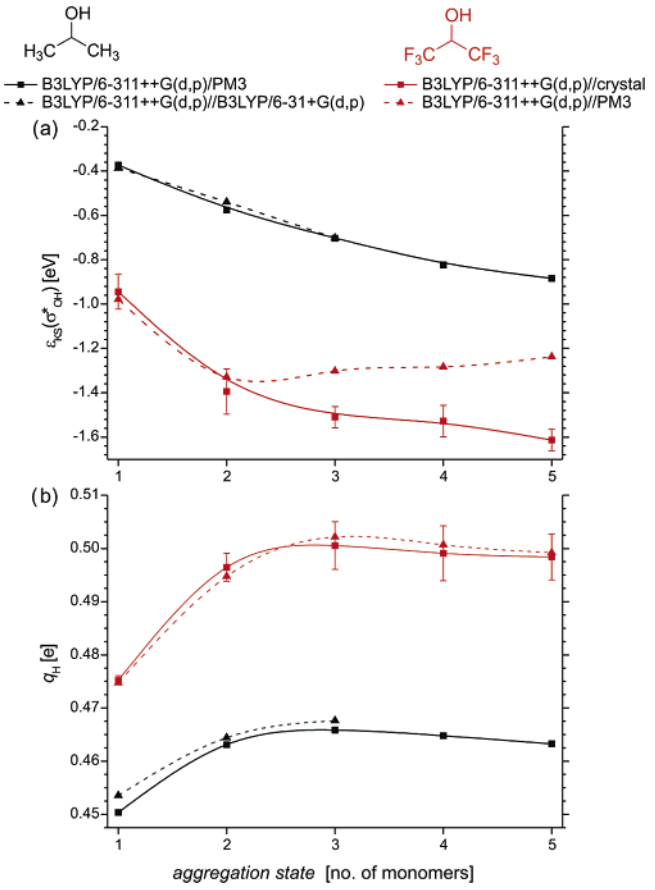

Figure 9. LUMO energy (σ^*_{OH}) (a) and natural charge q_H of the hydroxyl proton (b) vs aggregation state of HFIP.

(ii) constrained geometry optimizations refining only the position of the hydrogen atoms (denoted "//crystal" in Figure 9). In both cases, semiempirical PM3 was utilized.

2-Propanol: In helical HFIP structure fragments comprising up to five alcohol monomers, all fluorine atoms were substituted for hydrogen atoms. The resulting structures were subjected to unconstrained geometry optimizations using (i) PM3 and (ii) B3LPY/6-31+G(d,p), respectively.

The electronic structures of the resulting geometries were subsequently analyzed using B3LYP/6-311++G(d,p) single-point calculations. Partial atomic charges are based on an NBO-analysis.

Results of the Analysis of Alcohol Aggregates: For HFIP, a pronounced cooperativity in H-bond donor ability exists (Figure 9). The coordination of a second and a third molecule induces an enhanced polarization of the terminal hydroxyl group resulting in an increased partial charge q_H of the hydroxyl proton. This suggests an amplification of the electrostatic H-bond donor ability. Furthermore, the energy of the corresponding σ^*_{OH}-orbital decreases significantly upon dimerization and trimerization. In other words, aggregation results in an amplified potential to form H-bonds with a highly covalent character. These effects are approximately twice as pronounced for HFIP as compared to 2-PrOH (Figure 9). Aggregation beyond the trimers does not further enhance the H-bonding ability.

III. Summary and Conclusion

The most important results of our study can be summarized as follows:

(i) The reaction kinetics of the epoxidation of *Z*-cyclooctene with hydrogen peroxide in HFIP exhibit a second to third order dependence on the concentration of the fluoroalcohol.

(ii) In the condensed phase (liquid or solid), the sc (or even sp) conformation of HFIP is favored over the ap conformation.

(iii) The σ^*_{OH}-orbital energy of monomeric HFIP decreases and the dipole moment increases steadily and drastically upon rotation from the ap to the sp conformation.

(iv) Compared to the monomer, aggregates of 2 to 3 HFIP molecules show a pronounced decrease of the σ^*_{OH}-orbital energy and an increase of the positive partial charge at the terminal free hydroxyl group.

Two major conclusions can be drawn from the above results:

(i) The H-bond donor ability of monomeric fluorinated alcohols is highly dependent on the conformation along the CO-bond. Especially for HFIP, we expect the alcohol to adopt an sc or even sp conformation when it is to act as an H-bond donor. In any investigation of the influence of fluoroalcohol solvents on structure or reactivity, particular attention has to be paid to this effect, including the need to consider charge-transfer/orbital interaction. Any models relying exclusively on an electrostatic description of H-bonding may well lead to inadequate results.

(ii) Aggregates of HFIP, in particular dimers and trimers, need to be taken into account for proper mechanistic interpretations. Cooperative aggregation leads to enhanced H-bond donor ability. Thus, the neglect of aggregation will underestimate the potential of fluorinated alcohols as H-bond donors.

Acknowledgment. This work was supported by the Regional Computing Centre Cologne (RRZK) and by the Fonds der Chemischen Industrie (Kekulé-doctoral fellowship to J.A.A).

Supporting Information Available: Experimental procedures, complexation constants, full conformational analysis of monomeric PhTFE, X-ray crystal structure data, the full author list of ref 21, and the details of computed structures. This material is available free of charge via the Internet at http://pubs.acs.org.

JA0545463